The Total Core Losses in Bulk Amorphous Rods of $\mathrm{Fe_{60}Co_{10}Y_{8-x}Ni_{2+x}B_{20}}$ Alloys (Where $x = 0, 1$)

M. Nabiałek[a], B. Jeż[a,*], K. Jeż[a], S. Walters[b] and K. Błoch[a]

[a]Institute of Physics, Faculty of Production Engineering and Materials Technology,
Częstochowa University of Technology, al. Armii Krajowej 19, 42-200 Częstochowa, Poland

[b]Advanced Engineering Centre, School of Computing, Engineering and Mathematics, University of Brighton,
Cockcroft Building, Lewes Road, Brighton, BN2 4GJ, UK

As part of this work, structural investigations were carried out on rapidly-cooled alloys with the following chemical compositions: $\mathrm{Fe_{60}Co_{10}Y_{8-x}Ni_{2+x}B_{20}}$ (where $x = 0, 1$). X-ray diffraction studies confirmed that the tested materials have an amorphous structure. This structure is characterized by absence of long-range atomic order, in the contexts of angularity and periodicity. Therefore, these materials should exhibit different magnetic properties, compared with those of their crystalline counterparts. In the electrical power and electronics industries, there is a constant demand for materials with better and better properties. The main considerations of applicability are economics and environmental protection. The deciding parameter, determining the usefulness of ferromagnetic alloys in electrotechnical devices and considering economics and ecology, is their low losses on remagnetization. For the produced alloys, described in this paper, a series of loss tests for remagnetization at different frequencies was carried out. The losses for remagnetization — pertaining to the hysteresis loop — and additional losses were determined.

1. Introduction

The bulk amorphous materials are a relatively new group of functional materials. In contrast to the classic amorphous materials (thin ribbons [1–3], bulk alloys are produced at much lower cooling rates of 10^{-1}–10^3 K/s [4–7]. Materials with a thickness of at least 0.5 mm are considered to be bulk alloys. The lack of long-range atomic order generates different properties in these materials, in comparison to their crystalline counterparts.

The iron-based bulk amorphous alloys are a particularly interesting group of functional materials [8, 9]. Materials of this type are characterized by so-called soft-magnetic properties; i.e., a low coercive field value and high saturation of magnetisation [10–15]. This type of alloy can be used in the electronics and power industries, for example, as the core material of low-loss transformers. For application-related reasons, the important properties of these materials are their magnetic permeability and their losses for remagnetisation (core losses).

The total core losses [16, 17] for remagnetisation of a material consist of three factors: hysteresis losses P_{his}, eddy current losses P_{cl}, and additional losses P_{exc}:

$$P_t = P_{\mathrm{his}} + P_{\mathrm{cl}} + P_{\mathrm{exc}}. \tag{1}$$

Hysteresis losses are related to the surface of the dynamic magnetic hysteresis loop. The occurrence of hysteresis is associated with irreversible processes of remagnetisation, which is the result of the presence of centres that inhibit the movement of domain walls. An important component of remagnetisation losses are the losses associated with eddy currents; these arise during the magnetisation of the sample. The eddy currents create a field opposite to the applied magnetic field, thereby causing losses. Assuming a sinusoidal time-dependent induction waveform, the losses due to eddy currents can be described by the equation

$$P_{\mathrm{cl}} = \frac{\pi^2}{6} \sigma d^2 B_{\mathrm{peak}}^2 f^2, \tag{2}$$

where d is the thickness of the sample, σ is electrical conductivity, B_{peak} is the maximum value of the induction and f is frequency.

The last component, the so-called additional losses, can be expressed approximately by the equation [18]:

$$P_{\mathrm{exc}} = 8,76 \sqrt{\sigma G S V_0} B_{\mathrm{peak}}^{3/2} f^{3/2}, \tag{3}$$

where G is dimensionless factor, S is the cross-section area of the sample, V_0 is constant associated with the impact of pinning centres of the domain walls.

The occurrence of additional losses is associated with migration relaxation and so-called composition fluctuations.

The total core losses are closely related to the presence of the domain structure. In the case of crystalline materials (in which magnetocrystalline anisotropy occurs), the analysis of core losses allows a close correlation to be obtained between the domain structure and the losses. However, the complexity of the domain structure in amorphous alloys allows only a superficial determination of the chemical composition and microstructural connections with the level of core losses.

---

*corresponding author; e-mail: bartek199.91@o2.pl

It is assumed that, for the amorphous alloys, the main contribution to the loss is made by the field of the magnetic hysteresis loop. Due to the small cross-section of the samples and the high electrical resistance of amorphous materials, the losses associated with eddy currents are relatively low. The high resistance value is associated with the multicomponent nature of bulk amorphous alloys.

This study presents the results of investigations into the structure and magnetic properties of iron-based bulk amorphous alloys. The magnetic permeability and core losses of manufactured alloys were tested.

2. Experimental part

Polycrystalline alloys $Fe_{60}Co_{10}Y_{8-x}Ni_{2+x}B_{20}$ (where $x = 0, 1$), were prepared in an arc furnace. The experimental setup for the arc furnace is shown in Fig. 1.

Alloyed components with a purity of 99.98% were weighed to an accuracy of 0.0001 g. Ingots were made, each weighing 10 g. The melting process was carried out on a water-cooled copper plate. The component elements were melted using a plasma arc, the current flowing through the electrode being up to 400 A. In order to achieve the highest possible purity, the ingot was melted in the presence of a titanium getter, in order to capture the remaining impurities in the working chamber. The ingots were melted seven times, and they were physically inverted each time, thereby ensuring thorough mixing of the ingredients. The ingot production process was carried out under a protective atmosphere of argon. The ingots were divided into smaller pieces, and cleaned — both mechanically and using an ultrasonic cleaner. The batch material, prepared in this way, was used to produce a rapidly-cooled alloy using an injection-casting method, as shown in Fig. 2.

Each polycrystalline ingot was placed in a quartz crucible at the height of the copper coil. The alloy was melted using eddy current heating. The liquid alloy was injected under argon pressure into a water-cooled copper mould. The production process was carried out under a protective atmosphere of argon. The described injection-casting method allowed liquid alloy cooling rates of up to 10^3 K/s to be achieved. Rapidly-cooled alloys were produced in the form of rods, each with a diameter of 0.5 mm and a length of 30 mm. The rods were cleaned — both mechanically and using an ultrasonic cleaner.

The structure of the produced materials was examined using X-ray diffraction. A Bruker Advance D8 diffractometer, equipped with a Cu K_α lamp, was used for this part of the investigation. The tests were carried out on powdered material samples, over a 2Θ angle range of 30–100°. The exposure time of the samples was 5 s per measuring step (0.02°).

The magnetic properties of the produced materials were examined using a ferrometer, using the transformer method. The measurements were carried out at room
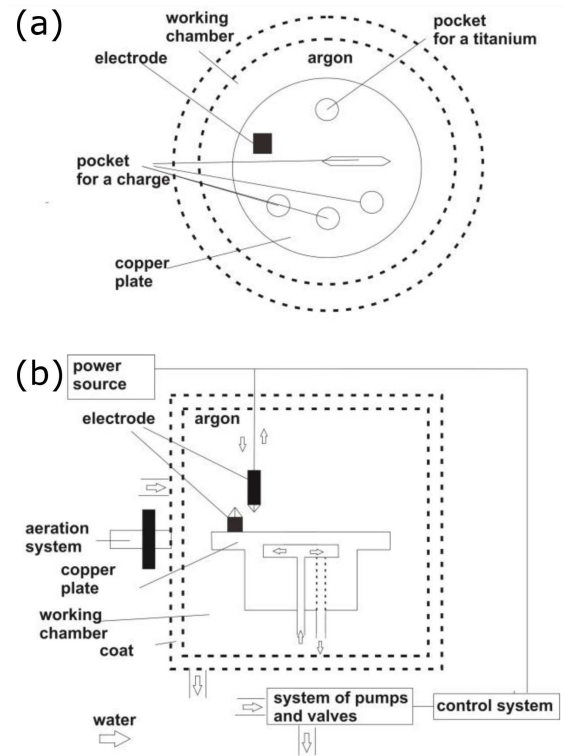

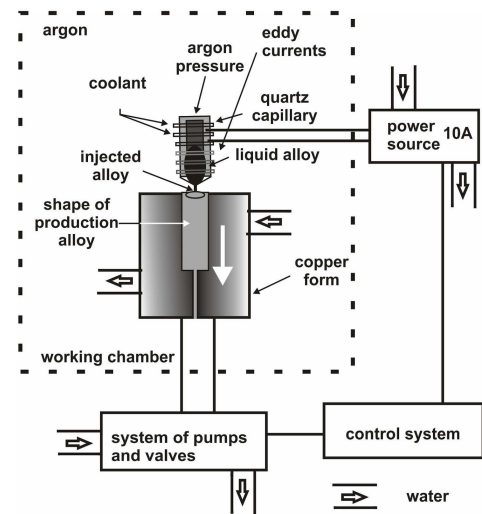Fig. 1.   The experimental setup for the arc furnace.

Fig. 2.   Production technique for the manufacture of rapidly-cooled alloys using an injection-casting method [19].

temperature. The alloy samples were placed in yokes made of super permalloy. The magnetic permeability of the created alloys, and the dynamic magnetic hysteresis loops, were measured. Total core losses also were determined. Additional losses were calculated, based on measurements. Measurements were carried out using a magnetic field frequency range of 50–1000 Hz.

3. Research results

Figure 3 presents X-ray diffraction spectra for the alloys produced.

The recorded diffractograms are typical of those normally obtained for amorphous materials [20]. In each case, only a single broad maximum is visible — in the 2Θ angle range of 40–50°. However, there is no visible peak from crystalline phases. Occurrence of each maximum is associated with the scattering of X-rays by chaotically-distributed atoms within the volume of the sample.

Figure 4 presents dynamic magnetic hysteresis loops recorded for the investigated alloys.

For amorphous alloys, exhibiting so-called soft magnetic properties, magnetic fields with an intensity of several tenths of H_c values have irreversible magnetisation processes [21]. This causes a magnetic hysteresis loop. The dynamic hysteresis loops, recorded as part of this investigation, are typical of those normally obtained for materials exhibiting soft magnetic properties [22]. The area of a hysteresis loop is a measure of losses for the remagnetisation of the sample. The area of the loop, and hence the magnitude of P_t, both increase with increasing frequency of the magnetising field. Figure 5 presents the relationship of the magnetic permeability with the amplitude of the magnetising field.

The $\mu(H)$ curves reveal the maximum that corresponds to the maximum permeability for each case. An increase in the amplitude of the magnetising field decreases the value of the resulting magnetic permeability. The magnetic permeability also decreases with increasing frequency of the magnetising field. For the alloy $Fe_{60}Co_{10}Y_8Ni_2B_{20}$, the maximum magnetic permeability is approximately 2400. The increased Ni content in the $Fe_{60}Co_{10}Y_7Ni_3B_{20}$ alloy causes a significant increase in permeability to approximately 3000, which is an expected result, due to the high magnetic permeability of Ni. In the case of the tested alloys, the maximum magnetic permeability occurs at similar values of amplitude of the magnetising field. Figure 6 shows core losses as a function of the maximum induction for the tested amorphous alloys.
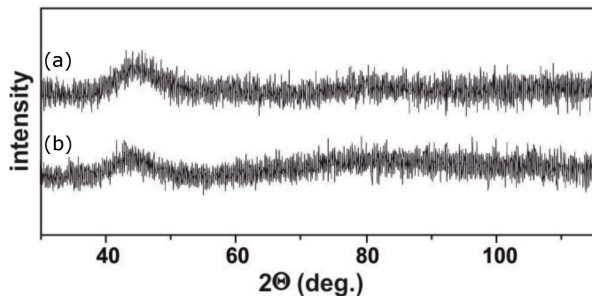

Fig. 3. X-ray diffraction spectra obtained for the investigated alloys: (a) $Fe_{60}Co_{10}Y_8Ni_2B_{20}$, (b) $Fe_{60}Co_{10}Y_7Ni_3B_{20}$.
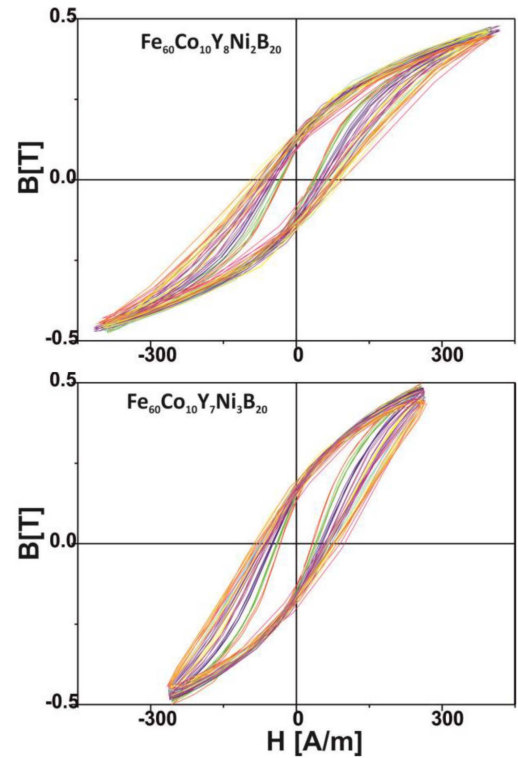

Fig. 4. Dynamic hysteresis loops, measured for the investigated alloys over a magnetic field frequency range of 50–1000 Hz.
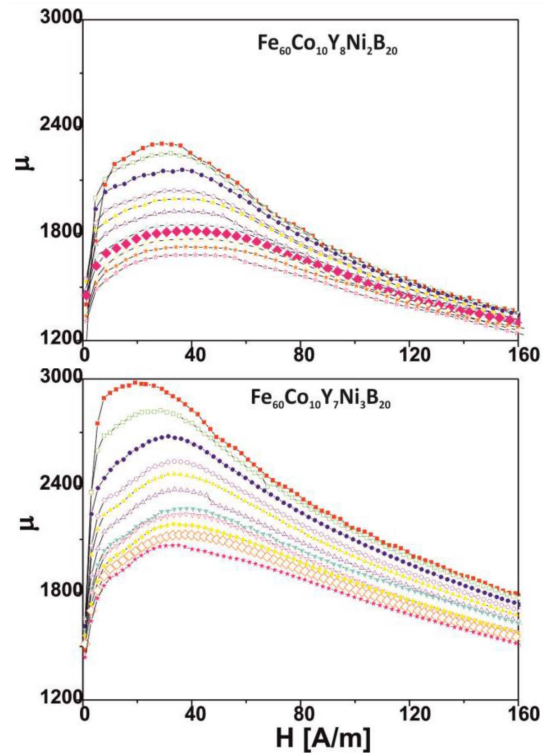

Fig. 5. Dependence of the magnetic permeability on the amplitude of the magnetising field; tested over a frequency range of 50–1000 Hz.
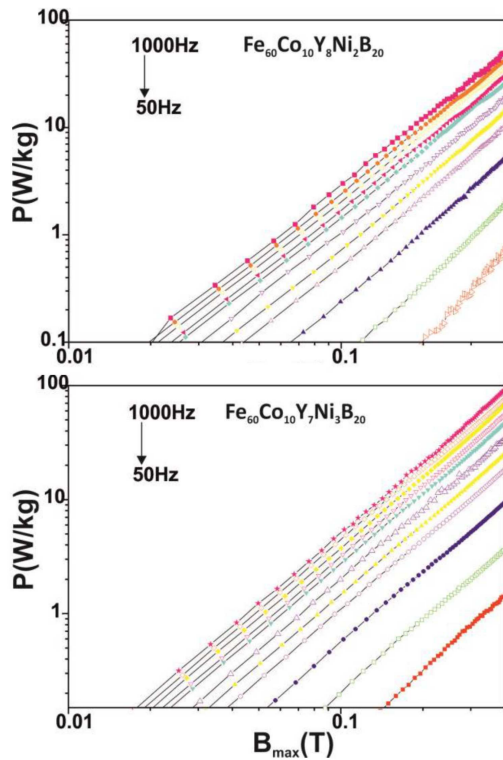
Fig. 6.   Core losses as a function of the maximum induction for the produced alloys; tested over a magnetic field frequency range of 50–1000 Hz.

Fig. 7.   Comparison of core losses (a) and dynamic magnetic hysteresis loops (b) for the produced alloys.

As mentioned previously, P_t are related to: the area of the magnetic hysteresis loop, eddy currents, and additional losses (composition fluctuations, magnetic delay). Bulk amorphous alloys are characterized by lower electrical resistance, compared to amorphous ribbons (due to their greater thickness). A higher conductivity value causes eddy currents and, consequently, an increase in losses associated with this component. Nevertheless, iron-based bulk amorphous alloys exhibit similar levels of core losses to those of classical Fe–Si sheets [23]. The value of core losses increases with increasing frequency of the magnetising field. Figure 7 presents the comparison of core losses and the dynamic magnetic hysteresis loops for the tested alloys.

Interestingly, the $Fe_{60}Co_{10}Y_8Ni_2B_{20}$ alloy is characterized by lower core losses, compared to the $Fe_{60}Co_{10}Y_7Ni_3B_{20}$ alloy. The increase in Ni content in the latter alloy caused a significant increase in the value of magnetic permeability. Therefore, the expected result should be lower core losses for this sample. The recorded dynamic magnetic hysteresis loops differ in shape. The $Fe_{60}Co_{10}Y_7Ni_3B_{20}$ alloy magnetises slightly more easily (it achieves a higher induction value at the same magnetising field). However, it achieves a higher remanence value.

It is worth noting that the surface areas of the loops for the tested alloys are almost identical. Hence, it is to be expected that higher core losses of the $Fe_{60}Co_{10}Y_7Ni_3B_{20}$
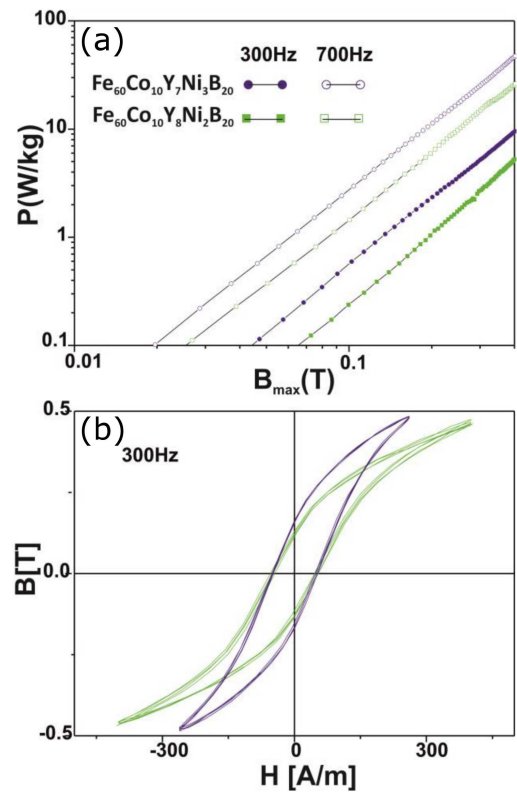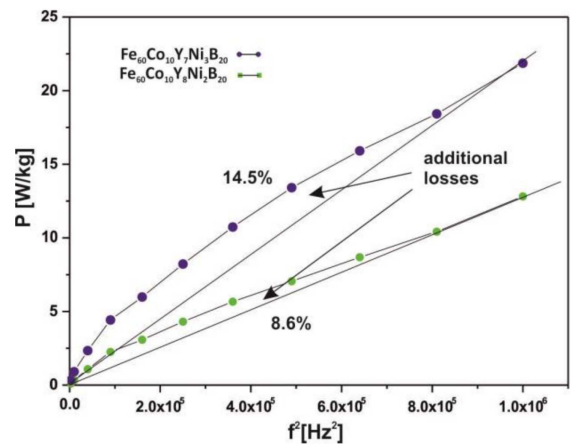

Fig. 8.   Core losses as a function of the square of the frequency of the magnetising field for tested alloys.

alloy may be associated with a lower value of electrical resistance, which causes an increase in losses from eddy currents. Figure 8 shows the core losses as a function of the square of the frequency of the magnetising field for the produced alloy samples.

The core losses should increase with the square of the frequency of the magnetising field. However, the determined losses are not a linear function of the square of the

frequency. This is due to the occurrence of P_{exc}, related to composition fluctuations and magnetic latencies. For the $Fe_{60}Co_{10}Y_8Ni_2B_{20}$ alloy, the contribution of P_{exc} is 8.6%, while for the alloy with higher Ni content, the P_{exc} amounts to 14.5%. Such a significant difference in the share of additional losses in the tested alloys can be explained by the presence of different degrees of disordered structure. It is hypothesized that a higher degree of heterogeneity may occur throughout the volume of the alloy with the higher Ni content — which would explain the higher share of additional losses (increased Ni content in bulk Fe-based alloys, especially those with a high Fe content, may affect glass forming ability — according to the experience of the research team). A higher value of core losses should be associated with a higher level of losses associated with eddy currents.

4. Conclusion

The aim of this study was to measure the core losses within samples of specially produced iron-based bulk amorphous alloys, and to determine the contribution of additional losses. Another objective of the work was to determine the effect of changes in chemical composition, both on the level of losses and on the magnetic permeability of the produced alloys. Based on the results of the research, the following conclusions were drawn:

- Bulk alloys with the chemical compositions: $Fe_{60}Co_{10}Y_{8-x}Ni_{2+x}B_{20}$ (where $x = 0, 1$) have an amorphous structure;

- An increase in Ni content results in a significant increase in the magnetic permeability value;

- Core losses as a function of frequency-squared are not a linear function. (Additional losses are a significant component of P_t.);

- Small changes in the Ni content, in the chemical composition of the alloy, have a significant impact on the level of P_t and on the share of additional losses (14.5% for the $Fe_{60}Co_{10}Y_7Ni_3B_{20}$ alloy and 8.6% for the $Fe_{60}Co_{10}Y_8Ni_2B_{20}$ alloy);

- The $Fe_{60}Co_{10}Y_7Ni_3B_{20}$ alloy, despite the higher value of magnetic permeability and similar surface area of the dynamic magnetic hysteresis loops, is characterized by much higher P_t. (This may be related to higher losses due to eddy currents).

Bulk amorphous alloys are characterized by a similar level of losses as those in the case of Fe–Si crystalline sheets. However, it should be said that the mechanism of core losses is more complicated than in the case of crystalline alloys. The occurrence of a rather complicated domain structure in amorphous materials makes it much harder to explain the mechanism of the exhibited losses. For these amorphous materials, the relationship between microstructure and the level of losses requires investigation. This is especially visible in the case of P_{exc}. Just a 1% substitution of Y with Ni caused a substantial difference in the percentage share of P_{exc}. This means that the magnetising process is closely related to the microstructure. In the case of amorphous materials, the decisive factor for resulting properties is the level of disordered structure. Local changes in the chemical composition and atomic packing density determine the level of core losses from the magnetic hysteresis loop as well as the additional losses.

References

[1] W. Li, Y.Z. Yang, J. Xu, *J. Non-Cryst. Solids* **461**, 93 (2017).

[2] J. Li, X. Wang, X. Liu, S. Zhao, K. Yao, *Physica B* **528**, 24 (2018).

[3] J. Gondro, *J. Magn. Magn. Mater.* **432**, 501 (2017).

[4] E.S. Park, H.K. Lim, W.T. Kim, D.H. Kim, *J. Non-Cryst. Solids* **298**, 15 (2002).

[5] Y. Geng, Y. Wang, Z. Wang, J. Qiang, H. Wang, C. Dong, O. Tegus, *Mater. Des.* **106**, 69 (2016).

[6] P. Pietrusiewicz, *Acta Phys. Pol. A* **133**, 666 (2018).

[7] M. Nabiałek, *J. Alloys Comp.* **642**, 98 (2015).

[8] M.E. McHenry, M.A. Willard, D.E. Laughlin, *Progr. Mater. Sci.* **44**, 291 (1999).

[9] M. Nabiałek, K. Jeż, *Rev. Chim.* **69**, 1593 (2018).

[10] Y. Geng, Z. Zhang, Z. Wang, Y. Wang, J. Qiang, C. Dong, H. Wang, O. Tegus, *J. Non-Cryst. Solids* **450**, 1 (2016).

[11] F. Wang, A. Inoue, Y. Han, F.L. Kong, S.L. Zhu, E. Shalaan, F. Al-Marzouki, A. Obaid, *J. Alloys Comp.* **711**, 132 (2017).

[12] X. Li, Z. Shi, T. Zhang, *J. Alloys Comp.* **784**, 1139 (2019).

[13] Y. Han, C.T. Chang, S.L. Zhu, A. Inoue, D.V. Louzguine-Luzgin, E. Shalaan, F. Al-Marzouki, *Intermetallics* **54**, 169 (2014).

[14] C. Dong, A. Inoue, X.H. Wang, F.L. Kong, E.N. Zanaeva, F. Wang, A.I. Bazlov, S.L. Zhu, Q. Li, *J. Non-Cryst. Solids* **500**, 173 (2018).

[15] J. Si, J. Mei, R. Wang, X. Chen, X. Hui, *Mater. Lett.* **181**, 282 (2016).

[16] R. Piccin, P. Tiberto, H. Chiriac, M. Baricco, *J. Magn. Magn. Mater.* **320**, 806 (2008).

[17] K. Bloch, M.A. Titu, A.V. Sandu, *Rev. Chim.* **68**, 2162 (2017).

[18] E. Barbisio, F. Fiorillo, C. Ragusa, *IEEE Trans. Magn.* **40**, 1810 (2004).

[19] B. Jeż, *Rev. Chim.* **68**, 1903 (2017).

[20] S. Garus, M. Nabiałek, J. Garus, *Acta Phys. Pol. A* **126**, 960 (2014).

[21] H. Kronmüller, T. Reininger, *J. Magn. Magn. Mater.* **112**, 1 (1992).

[22] M. Nabialek, J. Fuzer, L. Dakova, P. Pietrusiewicz, *Rev. Chim.* **68**, 1098 (2017).

[23] I. Ibarrondo, J. Degauque, *Vacuum* **53**, 75 (1999).